The 11th International Congress
Motor Vehicles & Motors 2026
Kragujevac, Serbia
October 8th - 9th, 2026

Motor Vehicles & Motors

MVM2026-001
https://doi.org/10.24874/CMVM2026.001
Original scientific paper

Miroslav Demić[1]
Mikhail P. Malinovsky[2]
Andrija Vujičić[3]

THEORETICAL-EXPERIMENTAL APPROACH TO THE DEVELOPMENT OF A METHOD FOR IDENTIFYING THE HEAT DISSIPATION RATE OF MOTOR VEHICLE SHOCK ABSORBERS

ABSTRACT: This paper develops and presents a methodological framework for analysing thermal loading of passenger vehicle shock absorbers under conditions of stochastic road excitation. In contrast to conventional approaches based on simplified quarter- or half-vehicle models, the study employs a spatial 7-DOF model, enabling precise simulation of coupled heave, pitch, and roll dynamics. The key scientific contribution of the paper is the introduction of a nonlinear shock absorber model, in which the force is defined as a function of relative velocity and relative displacement of the piston with respect to the body, thereby achieving a higher level of energy consistency compared to linear viscous models. By formulating the governing equations in the state-space domain, a direct link is established between numerical simulation and automatic control methods (system identification, spectral analysis, and Singular Value Decomposition - SVD), enabling identification of the frequency distribution of dissipated thermal power directly from experimental data. The analysis of the coupling between excitation signals and the thermal power generated in the shock absorbers indicates a strong influence of nonlinearity, as the partial coherence function is below approximately 0.25. Since these results were obtained through dynamic simulation, apart from the negligible influence of numerical methods, no additional noise sources were present; thus, the low values can be attributed to the nonlinear parameters of the vehicle oscillatory systems. On the other hand, the analysis of partial transfer functions shows that the highest thermal power of the shock absorbers is generated up to approximately 30 Hz. Considering the characteristics of nonlinear oscillatory systems, this is evidently a consequence of the resonant frequencies of sprung and unsprung masses. The developed method can also be applied in experimental investigations, where it is necessary to simultaneously measure forces and relative velocities of the piston with respect to the shock absorber body. The application of the SVD method enables a more detailed analysis of heat generation within the shock absorbers.

KEYWORDS: passenger vehicle, 7-DOF model, shock absorber, thermal power, stochastic excitation, system identification, SVD method

[1] *Miroslav Demić, Ph.D., retired professor, University of Kragujevac, Faculty of Engineering Kragujevac, Sestre Janjić 6, Kragujevac, Serbia, demic@kg.ac.rs , https://orcid.org/0000-0003-2168-1370*
[2] *Mikhail P. Malinovsky, Ph.D., Moscow Automobile and Road Construction State Technical University (MADI), Federal State Unitary Enterprise "Central Scientific Research Automobile and Automotive Engines Institute" (FSUE "NAMI"), Moscow, Russia, ntbmadi@gmail.com , https://orcid.org/0000-0001-7812-5653*
[3] *Andrija Vujičić, Ph.D., Centre for Research and Development Activities in the Automotive Industry (CIRD), Belgrade, Serbia, andrija.vujicic@cird.rs , https://orcid.org/0009-0008-9526-9972*

TEORIJSKO-EKSPERIMENTALNI PRISTUP RAZVOJU METODE ZA IDENTIFIKACIJU GENERISANE TOPLOTNE SNAGE AMORTIZERA MOTORNIH VOZILA

REZIME U radu je razvijen i predstavljen metodološki okvir za analizu toplotnog opterećenja amortizera putničkog vozila u uslovima stohastičke pobude puta. Nasuprot konvencionalnim pristupima koji koriste uprošćene modele četvrtine ili polovine vozila, u istraživanju je primenjen prostorni model sa sedam stepeni slobode (7-DOF), koji omogućava preciznu simulaciju spregnutih vertikalnih i ugaonih kretanja (galopiranje i valjanje). Ključni naučni doprinos rada predstavlja uvođenje nelinearnog modela amortizera, gde je sila definisana kao funkcija relativne brzine i relativnog pomeranja klipa u odnosu na telo, čime je postignuta viša energetska objektivnost u poređenju sa linearnim viskoznim modelima. Formulisanjem jednačina u prostoru stanja, uspostavljena je direktna veza između numeričke simulacije i metoda automatskog upravljanja (identifikacija sistema, spektralna analiza i SVD metoda), što omogućava identifikaciju frekventne raspodele disipirane toplotne snage neposredno iz eksperimentalnih podataka. Analiza podataka o sprezi signala pobude i toplotne snage koja se razvija u amortizerima pokazuje veliki uticaj nelinearnosti, jer je parcijalna funkcija koherence manja od oko 0,25. Kako su ovi rezultati dobijeni dinamičkom simulacijom, osim veoma malog uticaja numeričkih metoda, drugih šumova nije bilo, pa se njihove niske vrednosti mogu objasniti uticajem korišćenih nelinearnih parametara oscilatornih sistema vozila. Sa druge strane, analiza parcijalnih prenosnih funkcija je pokazala da se najveća toplotna snaga amortizera razvija do oko 30 Hz, a imajući u vidu karakteristike nelinearnih oscilatornih sistema, očigledno je da je to posledica rezonantnih učestanosti oslonjene i neoslonjenih masa. Razvijena metoda se može koristiti i tokom eksperimentalnih istraživanja, kada je neophodno istovremeno registrovati sile i relativne brzine kretanja klipa u odnosu na telo amortizera. Primenom metode SVD je moguća detaljnija analiza stvaranja toplote u njima.

KLJUČNE REČI: putničko vozilo, model sa sedam stepeni slobode, amortizer, toplotna snaga, stohastička pobuda, identifikacija sistema, SVD metoda.

INTRODUCTION

The dynamic behaviour of passenger vehicles under real road excitation conditions represents one of the most challenging problems in modern vehicle dynamics, as it directly affects ride comfort, stability, and structural durability (Gillespie, T. D. 1992; Savaresi, S. M. et al. 2010; Poussot-Vassal, C. et al. 2012; Genta, G. 2003; Milliken, W. F. & Milliken, D.L. 1995; Mitschke, M. & Wallentowitz, H. 2004; Crolla, D. A. 1988; Rajamani, R. 2005; Demić, M. 1997).

In the scientific literature, research often focuses on control strategies and the thermal stability of suspension systems (Rajamani, R. 2005; Demić, M. 1997; Demić, M. & Diligenski, B. 2018). In (Savaresi, S. M. et al., 2010), the design of semi-active suspension control systems is analysed in detail, emphasising the importance of adaptive algorithms for improving vehicle performance. Similarly, (Poussot-Vassal, C. et al., 2012) provides a comprehensive review of control strategies, highlighting the advantages of semi-active systems over passive ones in terms of energy efficiency and response.

The issue of heat generation within shock absorbers under random excitation is crucial for component durability. In (Demić, M. & Diligenski, Đ. 2018), the thermal behaviour of shock absorbers subjected to real operating conditions is investigated. For the identification of parameters of such systems, (Demić, M. & Belingardi, G. 2011; Ljung, L. 1999) provide a theoretical basis that enables precise definition of the behaviour of complex dynamic systems through mathematical models.

A particular contribution to the modelling of shock absorbers and their influence on vehicle performance is given in (Demić, M. & Diligenski, Đ. 2016), where numerical simulations of the thermal loading of shock absorbers in semi-active systems are specifically developed, directly correlating with the need for cooling optimisation.

Although simplified models (quarter-vehicle or half-vehicle) are often used in the literature for easier numerical treatment, they cannot adequately represent the spatial coupling of motions nor enable a precise assessment of the energy balance and thermal loading of shock absorbers under real conditions. The primary objective of this paper is the development and verification of a methodological framework which, based on an advanced spatial vehicle model, enables objective identification of the thermal power of shock absorbers (Demić, M. & Diligenski, Đ. 2016; Lang, G. H. et al., 2007). In contrast to conventional approaches, the proposed method is based on:

- a spatial model with seven degrees of freedom (7-DOF), encompassing vertical and angular motions (pitch and roll), thereby achieving high fidelity in simulating the real vehicle response (Demić, M. 1997),

- a nonlinear constitutive model of the shock absorber, in which the force is not solely a function of velocity but also of the relative displacement of the piston, ensuring the energy objectivity required for accurate quantification of dissipated heat (Demić, M. & Belingardi, G. 2011), and
- integration with automatic control methods, establishing a direct link between numerical simulations and real service life testing measurements (Doyle, J. C. et al., 1992; Tomović, R. et al., 1974).

By formulating the model in the state-space domain, the application of spectral analysis and the Singular Value Decomposition (hereinafter SVD) method is enabled for identifying the frequency distribution of thermal power directly from the vehicle model or from experimentally measured kinematic quantities and forces (Rotenberg, V. 1972; Demić, M. 2026). In this way, the paper goes beyond the scope of theoretical vibration analysis and offers a practical method applicable in real testing, thereby providing a systematic basis for optimising shock absorber design and their cooling systems under real operating conditions.

METHOD

Since the objective of this study was to define a method for assessing the thermal loading of shock absorbers under real conditions, it was considered appropriate to develop it using a spatial nonlinear vehicle model subjected to random vibrations due to motion over an uneven road surface. The developed method can also be applied during experimental investigations.

It is well known that, in practice, models of varying levels of complexity exist; however, the aim should always be to adopt a model of minimal structure that includes the parameters of interest for the analysis, as will be discussed further.

Vehicle vibratory model

The analysis is based on a spatial model of a passenger vehicle with seven degrees of freedom (7-DOF), which includes:

- vertical motion of the sprung mass,
- angular motions about the transverse and longitudinal axes (pitch and roll),
- vertical motions of the four unsprung masses (Demić, M. 1997).

In this way, simultaneous consideration of the coupled vertical–angular response and the individual dynamics of each wheel under spatially distributed stochastic road excitation is enabled. The geometric parameters (wheelbase, track width, positions of the centres of mass), masses, and moments of inertia are defined on the basis of a real vehicle.

The equations of motion are formulated using the Newton–Euler equations and expressed as a system of second-order differential equations, which, for numerical solution, are transformed into a system of first-order differential equations.

In contrast to the classical linear viscous model, in which the force is proportional to relative velocity, this study adopts an extended constitutive model of the shock absorber, ensuring the energy objectivity required for accurate quantification of heat dissipation, in which the force depends on (Demić, M. & Belingardi, G. 2011):

- the relative velocity between the piston and the housing,
- the relative displacement between the piston and the housing.

The mathematical relations will be presented later in the text. This formulation enables a more objective representation of the real behaviour of the shock absorber, particularly in regimes where nonlinear and hysteretic effects are present. From an energy perspective, it provides a direct link between the mechanical work of the force and energy dissipation in the form of heat.

It is emphasised that the aim of this paper is not to analyse the mechanisms of heat transfer and dissipation, but exclusively to quantify heat generation as a consequence of mechanical energy dissipation.

As is well known, a vehicle represents a spatial oscillatory system subjected to random vibrations due to macro- and micro-irregularities of the road surface, engine operation, wind effects, and similar disturbances (Gillespie, T. D. 1992; Savaresi, S. M. et al. 2010; Poussot-Vassal, C. et al. 2012; Genta, G. 2003; Milliken, W. F. & Milliken, D.L. 1995; Mitschke, M. & Wallentowitz, H. 2004; Crolla, D. A. 1988; Rajamani, R. 2005; Rotenberg, V. 1972).

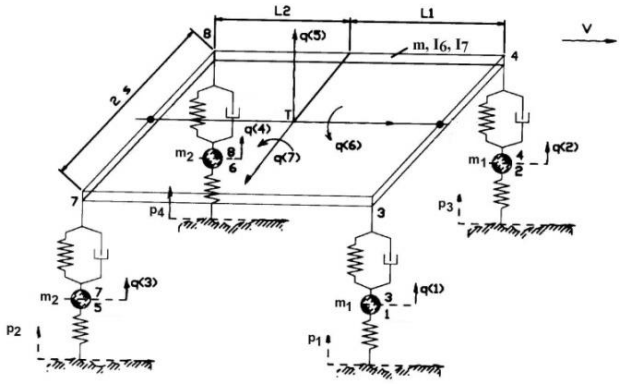


Figure 1 Vibratory model of the vehicle

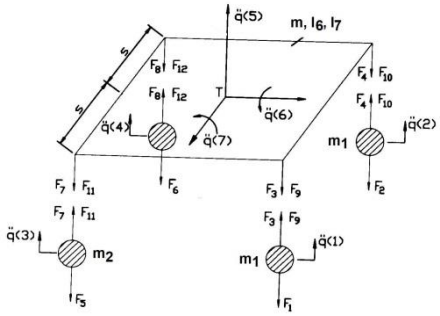


Figure 2 Forces acting on the adopted vehicle model

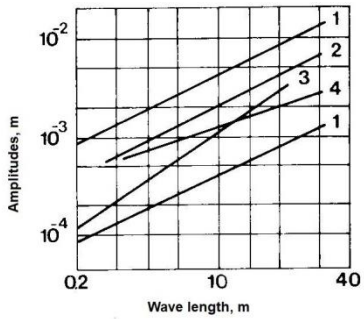


Figure 3 Amplitudes of road surface irregularities for modern roads:1 - limit values, 2 - road with poor concrete pavement, 3 - road with poor asphalt pavement, 4 - road with good asphalt pavement

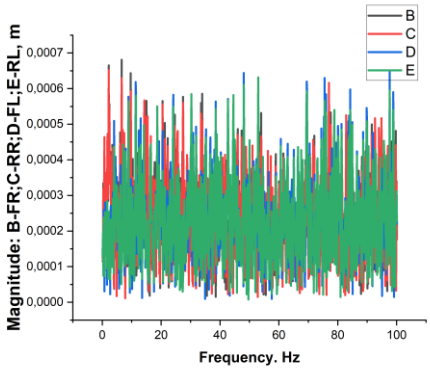


Figure 4 Excitation spectra at the wheels (B-front right; C-front left; D-rear right; E-rear left)

As is well known (Gillespie, T. D. 1992; Savaresi, S. M. et al. 2010; Poussot-Vassal, C. et al. 2012; Genta, G. 2003; Milliken, W. F. & Milliken, D.L. 1995; Mitschke, M. & Wallentowitz, H. 2004; Crolla, D. A. 1988; Rajamani, R. 2005; Rotenberg, V. 1972), a vehicle represents a spatial oscillatory system subjected to random vibrations under the influence of macro- and micro-irregularities of the road surface, engine operation, wind action, and similar disturbances. In the general case, since a vehicle consists of elastic elements, it possesses an infinite number of degrees of freedom of motion. As the analysis of such systems is extremely complex, a common simplification

assumes that the system consists of lumped masses interconnected by elastic–damping elements. In this case, each considered mass has six degrees of freedom of motion (Demić, M. 2026), and the motion of such systems can be described by the so-called Newton–Euler equations, Lagrange's differential equations of the second kind, and related formulations (Demić, M. 2026).

In the present case, a passenger motor vehicle with independent suspension at all four wheels and seven degrees of freedom (Figure 1) is considered (Demić, M. 2026). The vehicle moves in uniform rectilinear motion with velocity v, while the secondary oscillatory motions include vertical oscillations of the lumped wheel masses (four degrees of freedom), as well as vertical oscillations of the centre of mass of the sprung mass together with its angular motions of pitch and roll. Given that even such a system is difficult to analyse, it is considered appropriate to study small linear oscillations of the aforementioned masses about the vehicle's equilibrium position (Demić, M. 1997; Goldstein, H. et al. 2001). For clarity, the oscillatory model used in this study is briefly described below.

Based on the above considerations, Figure 1, and the simplification that the attachment points of the elastic–damping elements move along a chord rather than an arc (due to small angular displacements), the equations describing the deformations can be written as follows:

a) Springs

$$\begin{aligned} D_{1,2} &= q(5) + l_1 q(7) \mp sq(6) - q(1,2) \\ D_{3,4} &= q(5) + l_2 q(7) \mp sq(6) - q(3,4) \end{aligned} \tag{1}$$

b) Tyres

$$D_{4,5,6,7} = q(1,2,3,4) - p(1,2,3,4) \tag{2}$$

c) Relative velocities of the piston with respect to the shock absorber body

$$\begin{aligned} D_{9,10} &= \dot{q}(5) + l_1 \dot{q}(7)\, m\, s\, \dot{q}(6) - \dot{q}(1,2) \\ D_{11,12} &= \dot{q}(5) + l_2 \dot{q}(7)\, m\, s\, \dot{q}(6) - \dot{q}(3,4) \end{aligned} \tag{3}$$

Expressions (1–3) represent a standard linearised approximation of kinematic relations for small oscillations, which has been shown in the literature to be sufficient for analysing frequency characteristics of vehicle oscillatory systems.

Since the forces in the elastic–damping elements depend on the deformation of the elastic components and the relative velocity of the piston with respect to the shock absorber body, taking into account Figure 1 and expressions (1–3), and adopting the force characteristics given in (Demić, M. & Belingardi, G. 2011), the following relations can be formulated:

a) Tyres

$$\begin{aligned} F_{1,2} &= x(1)D_{5,6} + x(2)D^2_{5,6} - x(3)D^3_{5,6} \\ F_{5,6} &= x(4)D_{7,8} + x(5)D^2_{7,8} - x(6)D^3_{7,8} \end{aligned} \tag{4}$$

b) Springs

$$\begin{aligned} F_{3,4} &= x(7)D_{1,2} + x(8)D^3_{1,2} \\ F_{7,8} &= x(9)D_{3,4} + x(10)D^3_{3,4} \end{aligned} \tag{5}$$

c) Shock absorbers

$$\begin{aligned} F_{9,10} &= x(11) + x(12)D_{9,10} + x(13,14)sqr(D_{9,10})Sign(D_{9,10}) + \\ &\quad + x(15) + x(16)D_{1,2} + x(17)sqr(D_{1,2})Sign(D_{1,2}) \\ F_{11,22} &= x(18) + x(19)D_{9,10} + x(20,21)sqr(D_{11,12})Sign(D_{11,12}) + \\ &\quad + x(22) + x(23)D_{3,4} + x(24)sqr(D_{3,4})Sign(D_{3,4}) \end{aligned} \tag{6}$$

where:

- $x(1)$ to $x(24)$ – stiffness and damping parameters of the oscillatory system,

- $x(1)$ to $x(6)$– tyre stiffness parameters,
- $x(7)$, $x(8)$, $x(9)$, $x(10)$ – spring stiffness parameters,
- $x(11)$ to $x(24)$ – shock absorber damping parameters (where $x(13)$ and $x(20)$ refer to compression, and $x(14)$ and $x(21)$ to rebound of the shock absorber) (Demić, M. & Belingardi, G. 2011).

Based on Figure 2 and the Newton–Euler equations, after simplification, the differential equations describing the motion of the lumped masses of the vehicle can be written as follows:

a) Front right wheel

$$\ddot{q}(1) = (F_3 + F_9 - F_1) / m_1 \tag{7}$$

b) Front left wheel

$$\ddot{q}(2) = (F_4 + F_{10} - F_2) / m_1 \tag{8}$$

c) Rear right wheel

$$\ddot{q}(3) = (F_7 + F_{11} - F_5) / m_2 \tag{9}$$

d) Rear left wheel

$$\ddot{q}(4) = (F_8 + F_{12} - F_6) / m_2 \tag{10}$$

e) Vertical vibrations of the sprung mass

$$\ddot{q}(5) = -(F_3 + F_9 + F_4 + F_{10} + F_7 + F_{11} + F_8 + F_{12}) / m \tag{11}$$

f) Roll motion of the sprung mass

$$\ddot{q}(6) = (F_3 + F_9 + F_7 + F_{11} - F_4 - F_{10} - F_8 - F_{12}) s / I_6 \tag{12}$$

g) Pitch motion of the sprung mass

$$\ddot{q}(7) = [(F_7 + F_{11} + F_8 + F_{12}) l_2 - (F_3 + F_9 + F_4 + F_{10}) l_1] / I_7 \tag{13}$$

where:

- m_1, m_2, m_3, m_4 – masses of the wheels and associated assemblies,
- m – sprung mass of the vehicle (body),
- I_6– moment of inertia about the longitudinal axis of symmetry of the sprung mass,
- I_7– moment of inertia about the transverse axis of symmetry of the sprung mass,
- q_1, q_2, q_3, q_4 – vertical displacements (vibrations) of the wheels,
- q_5, q_6, q_7 – vertical displacement of the sprung mass and its roll and pitch motions,
- $\ddot{q}_1, \ddot{q}_2, \ddot{q}_3, \ddot{q}_4$ – accelerations of the vertical vibrations of the wheels,
- $\dot{q}_5, \dot{q}_6, \dot{q}_7$ – velocities of the vertical vibration of the sprung mass and its roll and pitch motions,
- $\ddot{q}_5, \ddot{q}_6, \ddot{q}_7$ – accelerations of the vertical vibration of the sprung mass and its roll and pitch motions,
- s – half-track of the wheels and tyres (for simplicity, it is assumed to be the same for both axles), and
- l_1, l_2 – coordinates of the centre of gravity of the sprung mass measured from the front and rear axles, respectively.

Table 1 Vehicle inertial parameters

m_1= 27.5, kg	I_7=53, kgm^2
m_2=25, kg	l_1=1.4, m
m=1090, kg	l_2=1.1, m
I_6=1680, kgm^2	s=0.7, m

The excitation function can be defined based on standard curves (ISO 8608, 2016). However, analyses have shown that these curves do not allow direct definition of the road excitation function in the time domain; therefore, it was considered appropriate to use the curves shown in Figure 3 (Rotenberg, V. 1972). With this in mind, it is

assumed that the excitation at the wheels is polyharmonic with real-valued amplitudes. The expression defining the excitation at the front right wheel is given in (Demić, M. 1997):

$$p_1(t) = \sum_1^{NH} A(f)\sin[(2\pi ft + \theta(f)] \tag{14}$$

where:

- A(f) – amplitude spectrum of road micro-irregularities (Figure 3),
- f – frequency,
- NH – number of harmonics, and
- θ – phase angle.

In the absence of experimental data, the following relation is adopted:

$$\theta(f) = 2\pi(RND - 0.5) \tag{15}$$

where RND denotes a random variable uniformly distributed in the interval {0,1}.

Table 2 Vehicles vibratory parameters

Parameter	Value
x(1), N/m	60000
x(2), N/m^2	47000
x(3), N/m^3	19000
x(4), N/m	60000
x(5), N/m^2	39000
x(6), N/m^3	22000
x(7), N/m	23000
x(8),N/m^3	6500
x(9), N/m	35000
x(10), N/m	67000
x(11), N	67.51
x(12), Ns/m	-3.17
x(13), Ns^2/m^2	0.0028
x(14), Ns^2/m^2	-2.10
x(15), N	-0.0077
x(16), N/m	-2.10
x(17), N/m^2	0.057
x(18), N	87.75
x(19), Ns/m	-4.12
x(20), Ns^2/m^2	0.0036
x(21), Ns^2/m^2	-2.73
x(22),N	0.0101
x(23), N/m	-2.73
x(24), N/m^2	0.074

The dependence of the excitation amplitude on vehicle speed is given by the expression (Demić, M. 1997):

$$A(f_p) = (A_0 + B_0 / f_p) / V \tag{16}$$

where:

- A_0, B_0 – ordinates taken from Figure 3,
- f_p – reciprocal value of the wavelength of road irregularities (Figure 3),
- v – vehicle speed.

The excitation acting on the rear right wheel is defined as:

$$p_3(t) = p_1(t - L / V) \tag{17}$$

To define the excitations on the left-hand side of the vehicle, it is assumed that they possess a different frequency content and include a time delay relative to the right-hand side.

Taking into account that in (Demić, M. 2026) the excitation function at all wheels is described in detail (neglecting the influence of tyre elasticity and wheel diameter), it was considered appropriate here to perform a frequency analysis of the wheel excitations. The magnitudes of the spectra are shown in Figure 4, it can be observed that the spectra are random functions of frequency.

Thermal loading of shock absorbers

The mechanical work realised in shock absorbers through the action of relative velocities and damping forces is entirely dissipated in the form of heat. The instantaneous power of dissipation in a damping element is equal to the product of the damping force and the relative velocity between the connected masses (Bojić, M. 2011; Atkins, P. 2010). Since the damping force is a function of relative velocity, the dissipated power has a distinctly non-linear character and directly depends on the oscillatory regime of the vehicle system.

This approach enables a direct link between the dynamic behaviour of the vehicle and the thermal loading of the shock absorbers.

In the present case, the thermal power is calculated using the expression:

$$P_{tp} = F_d \, v_{rel} \tag{18}$$

where:

- F_d – damping force in the corresponding damping element, and
- v_{rel} – corresponding relative velocity calculated from (1).

Considering the nature of the solutions of the differential equations (3), it is evident that the thermal power will also be of a random character, which will be discussed later.

Connection with automatic control methods

Given that the objective was to develop a method applicable in experimental investigations, the formulation of the model in the state-space domain enables the direct application of methods from automatic control and system identification. Based on measured quantities (shock absorber forces and relative velocities), it is possible to:

- estimate transfer functions between road excitation and dissipated power,
- determine the spectral distribution of generated heat,
- identify the parameters of the shock absorber constitutive model.

In this way, the developed methodology goes beyond purely numerical simulation and becomes applicable in operational and experimental studies.

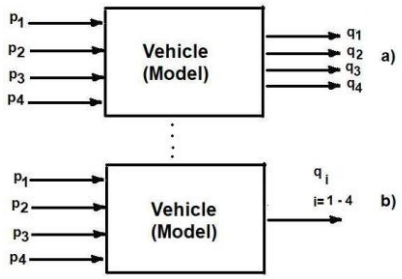


Figure 5 Procedure for solving a MIMO system by decomposition into multiple MISO subsystems

Since it is both desirable and useful to apply automatic control procedures during experimental investigations (Doyle, J. C. et al., 1992; Tomović, R. et al. 1974), one possible approach will be briefly outlined. The influence of wheel excitations and the generated thermal power can be represented as a multiple-input, multiple-output (MIMO) system (Figure 5a). The solution of such systems is based on reducing the MIMO system to multiple inputs and a single output (Figure 5b), where the input variables should be mutually independent. As the excitations in this case are not independent, decoupling methods must be applied (Demić, M. 2026). Since their application to this vehicle model has been described in detail in (Demić, M. 2026), and the same excitations are used here, it will not be discussed further. It is emphasised that the SVD method has been employed.

The proposed method integrates:

- a spatial dynamic vehicle model,
- a realistic constitutive model of the shock absorber,
- an energy-based formulation of dissipation, and

- spectral analysis and system identification.

This establishes a unified framework for quantifying the generation of thermal power in shock absorbers as a function of excitation frequency under real operating conditions of a vehicle travelling over an uneven road surface.

It should be noted that the system of first-order differential equations was solved numerically using the Runge–Kutta method, with an integration step of 0.001, s, over 16,384 points. This enabled reliable analysis in the frequency range from 0.06 Hz to 500 Hz (Bendat, J. & Piersol, A. 2000; Bendat, J. & Piersol, A. 2011). Considering that the resonant frequencies of the lumped masses of motor vehicles are approximately within the range 1 Hz – 25 Hz (Mitschke, M. & Wallentowitz, H. 2004), it was deemed appropriate to analyse only the frequency range 0.06 Hz – 100 Hz.

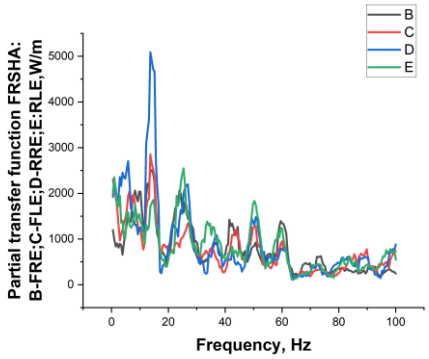


Figure 6 Partial transfer function: front right shock absorber – road excitations (FRE – front right wheel, RRE – rear right wheel, FLE – front left wheel, RLE – rear left wheel)

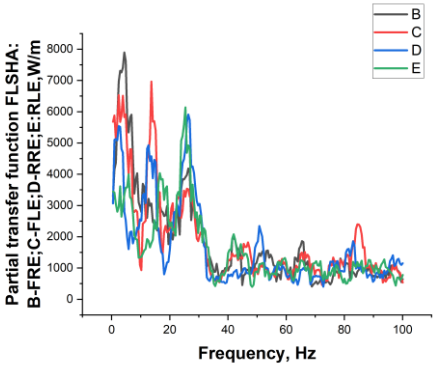


Figure 7 Partial transfer function: front left shock absorber – road excitations (FRE – front right wheel, RRE – rear right wheel, FLE – front left wheel, RLE – rear left wheel)

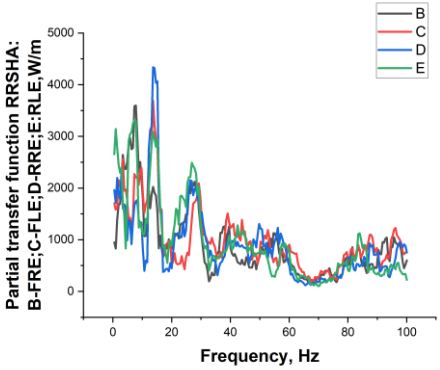


Figure 8. Partial transfer function: rear right shock absorber – road excitations (FRE – front right wheel, RRE – rear right wheel, FLE – front left wheel, RLE – rear left wheel)

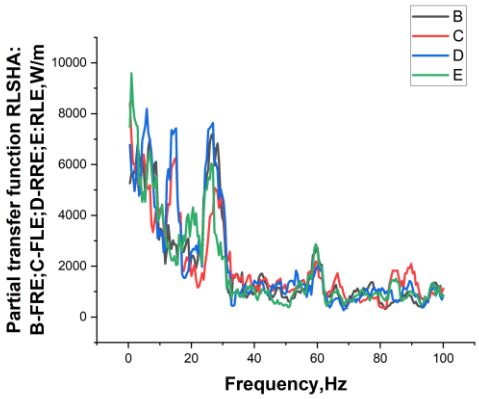


Figure 9 Partial transfer function: rear left shock absorber – road excitations (FRE – front right wheel, RRE – rear right wheel, FLE – front left wheel, RLE – rear left wheel)

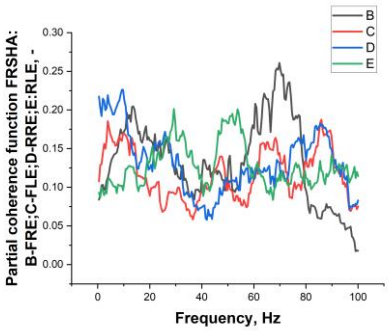


Figure 10 Partial coherence function: front right shock absorber – road excitations (FRE – front right wheel, RRE – rear right wheel, FLE – front left wheel, RLE – rear left wheel)

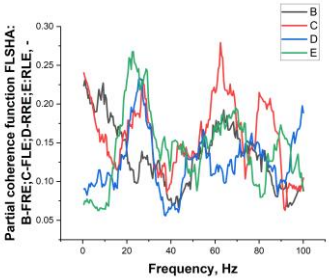


Figure 11 Partial coherence function: front left shock absorber – road excitations (FRE – front right wheel, RRE – rear right wheel, FLE – front left wheel, RLE – rear left wheel)

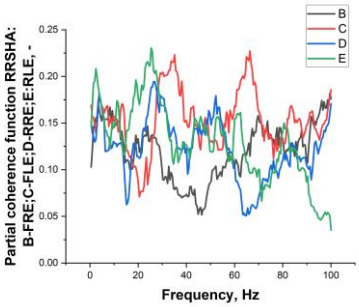


Figure 12 Partial coherence function: rear right shock absorber – road excitations (FRE – front right wheel, RRE – rear right wheel, FLE – front left wheel, RLE – rear left wheel)

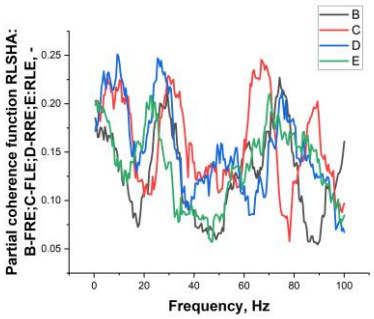


Figure 13 Partial coherence function: rear left shock absorber – road excitations (FRE – front right wheel, RRE – rear right wheel, FLE – front left wheel, RLE – rear left wheel)

DATA ANALYSIS

Analysis of the data presented in Figures 6–9 indicates that the generated thermal power depends on the position of the shock absorber. The rear wheels, particularly on the left-hand side, exhibit significantly higher peak values, reaching nearly 10,000 W/m, whereas the maxima at the front wheels are generally below 8000 W/m. This suggests that the rear part of the system is subjected to greater thermal loading in the low-frequency range, which is often a consequence of mass distribution or suspension stiffness.

An asymmetry between the left and right sides is also observed. For example, the left-hand side (FLSHA and RLSHA) shows higher values at the very beginning (close to 0 Hz) compared to the right-hand side. This difference in the initial part of the curves may indicate an uneven distribution of loads or different damping characteristics between the left and right sides of the model.

It is also of interest to analyse the positions of the resonant frequencies.

From Figure 6, resonant frequencies can be observed up to approximately 1.95 Hz, followed by a second resonance in the range 5.85 Hz – 6.34 Hz, and a third in the range 23.92 Hz – 25.39 Hz. At higher frequencies, the amplitudes of the transfer functions decrease (due to system nonlinearity).

Figure 7 shows resonant frequencies in the range 2.44 Hz –4.39 Hz, followed by a second resonance between 10.74 and 13.67 Hz, and a third in the range 22.46 Hz – 25.39 Hz. At higher frequencies, the amplitudes again decrease (as a result of system nonlinearity).

From Figure 8, resonant frequencies are identified in the range 2.92 Hz –3.41 Hz, followed by a second resonance between 9.27 Hz and 9.76 Hz, and a third in the range 25.87 Hz – 28.32 Hz. At higher frequencies, the amplitudes decrease due to nonlinear effects.

Figure 9 shows resonant frequencies up to 2.92 Hz, followed by a second resonance between 4.39 Hz and 6.83 Hz, and a third in the range 22.46 Hz – 24.41 Hz. At higher frequencies, the amplitudes of the transfer functions decrease (again due to system nonlinearity).

A common feature of all the analysed figures is that the transfer functions depend on frequency. Since a nonlinear vehicle model is considered, multiple peaks appear in the transfer functions. The lowest frequencies can be associated with the resonance of the sprung mass, while the higher ones correspond to the resonances of the wheels.

As is well known (Bendat, J. & Piersol, A. 2000; Bendat, J. & Piersol, A. 2011), partial coherence functions indicate the degree of linear correlation between two signals, i.e. whether nonlinearities or noise significantly influence the system.

When analysing partial coherence functions, it should be borne in mind that nonlinear oscillatory parameters of the vehicle were used and that noise arises only from minimal numerical errors.

The coherence values in Figures 10–13 are relatively low (below 0.30), which in signal analysis theory often indicates that the system is nonlinear, or that there is a significant influence of noise, or that the analysed partial inputs do not fully capture all causes of variation in the output signal.

It is observed that the partial coherence functions depend on both frequency and the position of excitation (front–rear and left–right sides of the vehicle), which indicates the complexity of the transformation of mechanical work into generated thermal power in the shock absorbers.

Considering that the partial coherence functions are low, this confirms that the system is nonlinear, and that only negligible noise is present, originating from the applied numerical methods.

From Figure 10, it can be determined that the minimum value of the partial coherence function occurs for the rear right wheel (41.99 Hz - 0.057), while the maximum value occurs for the front right wheel (68.84 Hz - 0.253).

From Figure 11 (front left wheel), the minimum value occurs at approximately (37.59 Hz - 0.055), while the maximum occurs for excitation at the front left wheel (62.50 Hz - 0.279).

In Figure 12, the maximum value occurs for the rear left wheel (27.34 Hz - 0.206), while the minimum occurs for excitation at the rear right wheel (66.40 Hz - 0.054).

From Figure 13, it can be seen that the maximum value occurs for the rear right wheel (9.27 Hz - 0.251), while the minimum occurs for excitation at the front right wheel (89.35 Hz - 0.054).

It should be noted that under real operating conditions, coherence rarely reaches ideal values due to tyre hysteresis and the progressive characteristics of springs.

It can therefore be concluded that the partial coherence functions of all shock absorbers depend on both frequency and excitation position, which must be taken into account when planning and interpreting experimental investigations.

Finally, it is emphasised that the developed method has been illustrated using a nonlinear vehicle model, but it is of general significance, as it can be applied in experimental testing of vehicles. In such cases, thermal power can be calculated based on measured shock absorber forces and the relative velocities of the piston with respect to the body.

CONCLUSIONS

The conducted research on the development of a method for identifying the thermal power of shock absorbers enables the following conclusions to be drawn:

- necessity of spatial modelling: the use of a 7-DOF model is justified, as only such an approach can capture the complex longitudinal and diagonal dynamic coupling between the wheels, which directly affects the distribution of thermal loading within the suspension elements.
- refinement of the shock absorber model: abandoning the linear viscous representation and introducing force dependence on both relative velocity and piston displacement is essential for a physically consistent estimation of instantaneous and mean thermal power.
- identification of dominant frequencies: a critical frequency range has been identified, corresponding to the resonant frequencies of the considered lumped masses of the system, within which maximum dynamic amplification and intensive energy dissipation occur, regardless of the primary location of excitation.
- specificity of energy transfer: the analysis has shown that maximum thermal loads may occur in shock absorbers that are not directly subjected to the primary excitation (e.g. diagonally opposite wheels), which is of crucial importance for fatigue analysis and the thermal stability of the shock absorber oil.
- experimental applicability: the proposed method, based on automatic control procedures (MIMO and MISO systems), successfully bridges the gap between theoretical simulations and measurements under real operating conditions, enabling identification of the energy balance based on standard measurable kinematic quantities.

This methodology provides a foundation for further research in the field of thermal loading of vehicle suspension systems, particularly in high-performance vehicles and heavy-duty trucks, where the shock absorber “fading” effect represents a critical safety factor.

REFERENCES

Atkins, P. (2010). *The laws of thermodynamics: a very short introduction*. Oxford University Press, Oxford. https://doi.org/10.1093/actrade/9780199572199.001.0001

Bendat, J., & Piersol, A. (2000). *Random Data: Analysis and Measurement Procedures (3rd ed.)*. John Wiley & Sons, New York/LondonISBN: 978-0471317302.

Bendat, J. S., & Piersol, A. G. (2011). Random Data: Analysis and Measurement Procedures (4th ed.). John Wiley & Sons, Hoboken, NJ. https://doi.org/10.1002/9781118032428

Bojić, M. (2011). *Thermodynamics (Termodinamika)*. Faculty of Engineering Sciences, Kragujevac. ISBN: 978-86-81037-34-8.

Crolla, D. A. (1988). Vehicle dynamics — theory into practice. *Proceedings of the Institution of Mechanical Engineers, Part D: Transport Engineering*, 202(2), 83–94. https://doi.org/10.1243/PIME_PROC_1996_210_250_02

Demić, M. (1997). *Optimization of motor vehicle oscillatory systems (Optimizacija oscilatornih sistema motornih vozila)*. Faculty of Mechanical Engineering, Kragujevac. ISBN: 86-80581-22-2

Demić, M. (2026). Contribution to the research of the influence of coherent random road excitations on the frequency characteristics of passenger motor vehicle vibrations. *Science Journal of Transportation*, 25(1), 19-37.

Demić, M., & Belingardi, G. (2011). A Contribution to shock absorber modelling and analysis of their influence on vehicle ride characteristics. *Journal of Middle European Construction and Design of Cars (MECCA)*, 9(1), 6-17. https://doi.org/10.2478/v10138-011-0002-4

Demić, M., & Diligenski, Đ. (2016). Numerical simulation of shock absorbers heat load for semi-active vehicle suspension system. Thermal Science, 20(5), 1725–1739. https://doi.org/10.2298/TSCI150624005D

Demić, M., & Diligenski, Đ. (2018). A contribution to the study of thermal loads of hydraulic and active mounts of powertrain of a freight motor vehicle. *Journal of Applied Engineering Science*, 16(2), 217–224. https://doi.org/10.5937/jaes16-15905

Doyle, J. C., Francis, B. A., & Tannenbaum, A. R. (1992). *Feedback control theory*. Macmillan Publishing Company, NY. ISBN: 978-0023305511.

Genta, G. (2003). *Motor vehicle dynamics: modeling and simulation*. World Scientific Publishing. https://doi.org/10.1142/3329

Gillespie, T. D. (1992). *Fundamentals of vehicle dynamics*. SAE International, Warrendale, PA. https://doi.org/10.4271/R-114

Goldstein, H., Poole, C. P., & Safko, J. L. (2001). *Classical Mechanics (3rd Edition)*. Addison-Wesley. ISBN: 978-0201657029.

ISO 8608 (2016). Mechanical vibration — Road surface profiles — Reporting of measured data. International Organization for Standardization, Geneva. 30 pages.

Lang, G. H., et al. (2007). Development of Suspension Design Technology Applying Principal Elastic Axes. *SAE Technical Paper*, 2007-01-0857. https://doi.org/10.4271/2007-01-0857

Ljung, L. (1999). System Identification: Theory for the User (2nd ed.). Prentice Hall, Upper Saddle River, NJ. ISBN: 978-0136566953

Milliken, W. F., & Milliken, D. L. (1995). *Race car vehicle dynamics*. SAE International, Warrendale. ISBN: 978-1560915263

Mitschke, M., & Wallentowitz, H. (2004). *Dynamik der kraftfahrzeuge (motor vehicle dynamics)*. Springer-Verlag, Berlin. https://doi.org/10.1007/978-3-662-06802-1

Poussot-Vassal, C., Sename, O., Dugard, L., & Gáspár, P. (2012). A survey on semi-active suspension control strategies. *Vehicle System Dynamics*, 50(2), 221–247. https://doi.org/10.3182/20110828-6-IT-1002.00446

Rajamani, R. (2006). *Vehicle dynamics and control*. Springer Science+Business Media, NY. https://doi.org/10.1007/0-387-28823-6

Rotenberg, V. (1972). Vehicle suspension (Podveska avtomobilya). Mashinostrojenie, Moscow. (In Russian).

Savaresi, S. M., Poussot-Vassal, C., Spelta, C., Sename, O., & Dugard, L. (2010). *Semi-active suspension control design for vehicles*. Elsevier (Butterworth-Heinemann), Oxford. https://doi.org/10.1016/C2009-0-63839-3

Tomović, R., Vukobratović, M., & Rakić, R. (1974). Introduction to Nonlinear Automatic Control Systems (Uvod u nelinearne sisteme automatskog upravljanja). Naučna knjiga, Belgrade.